

## X-ray magnetic-circular-dichroism study of Fe/V multilayers

G. R. Harp\* and S. S. P. Parkin

*IBM Research Division, Almaden Research Center, 650 Harry Road, San Jose, California 95120-6099*

W. L. O'Brien

*Synchrotron Radiation Center, University of Wisconsin-Madison, 3731 Schneider Drive, Stoughton, Wisconsin 53589*

B. P. Tonner

*Synchrotron Radiation Center, University of Wisconsin-Madison, 3731 Schneider Drive, Stoughton, Wisconsin 53589  
and Department of Physics, University of Wisconsin-Milwaukee, 1900 East Kenwood Boulevard, Milwaukee, Wisconsin 53211*

(Received 12 October 1994; revised manuscript received 10 November 1994)

The x-ray magnetic circular dichroism (XMCD) at the Fe and V  $2p$  edge is measured in Fe/V multilayers. For a V  $3 \text{ \AA}/\text{Fe } 4.4 \text{ \AA}$  multilayer, the induced V moment is at least  $0.26\mu_B$ , and it is aligned antiferromagnetically with the Fe layers. The V dichroism signal is revealed to have a complicated structure relative to, e.g., the Fe dichroism signal. We estimate the orbital moment on the V to be  $0.13\mu_B$ , similar to values seen in other ferromagnetic first-row transition metals. Only a lower bound for the V spin moment can be determined ( $0.13\mu_B$ ), due to the breakdown of the XMCD spin "sum rule" in the case of V.

Several unusual magnetic properties are observed in artificially layered ferromagnetic/nonmagnetic structures, such as oscillatory interlayer exchange coupling.<sup>1</sup> An important key to understanding such effects is to learn what is the magnetic response of the nonmagnetic layer when it is in contact with the ferromagnetic (FM) layers. However, the small induced magnetization developed in the nonmagnetic (NM) layers is usually swamped by the much larger magnetization of the adjacent FM layers, so that it is usually necessary to employ an element specific probe to determine the magnetic state of the NM layer.<sup>2</sup> One way to achieve element specificity is through the use of a highly surface sensitive probe. Then the induced magnetism in the surface layer (say, a NM film) may be probed independently from the FM bulk. But to probe true multilayer structures, one needs chemical selectivity, such as in x-ray magnetic circular dichroism (XMCD). Here we apply XMCD to determine the induced V magnetic moment in a Fe/V multilayer.

Oscillatory interlayer exchange coupling as a function of V layer thickness has been reported in sputtered Fe/V multilayers,<sup>3</sup> making it a good candidate for study of the NM layer induced magnetization. The Fe/V system is also interesting because calculations indicate different behavior for V films on Fe compared with V in Fe/V multilayers. A theoretical study<sup>4</sup> indicates layer by layer antiferromagnetism in V films on Fe, with the initial V monolayer (ML) antiferromagnetically aligned with the Fe and having a magnetic moment of  $-1.7\mu_B$  per atom. In contrast, the same study showed an induced moment of only  $-0.82\mu_B$  per atom for the V ML and  $-0.23\mu_B$  per atom for the V bilayers sandwiched between Fe layers.

An experimental study of thin V films on Fe using spin-polarized electron energy loss spectroscopy<sup>5</sup> (a surface sensitive probe) generally agrees with the above prediction, finding an induced V moment of  $\leq 1\mu_B$  for 0.8 ML V films, followed by layer by layer antiferromagnetism. In the present study, we focus on a multilayer film with the structure

Si(100)/Fe  $55 \text{ \AA}/[\text{Fe } 4.4 \text{ \AA}/\text{V } 3 \text{ \AA}]_{20}/\text{Fe } 22 \text{ \AA}$ . This V thickness corresponds to 1.5–2 ML of V in this polycrystalline film, which should present a good comparison to the above-mentioned calculations and experiment. Note that each V atom is in contact with at least one Fe layer, so the V should show high polarization. This particular film showed ferromagnetic coupling between adjacent Fe layers, so that all V layers are in similar environments.

The samples reported here were deposited by magnetron sputtering in  $3.25 \times 10^{-3}$  Torr Ar, with a deposition rate of  $2 \text{ \AA}/\text{s}$ . The base pressure of this system is about  $1 \times 10^{-8}$  Torr. The samples were transported in air to the synchrotron radiation center in Madison, WI, and pieces of them were inserted into a UHV chamber (base pressure  $1 \times 10^{-10}$  Torr) for XMCD measurements. Samples were magnetized *in situ* in 2 kOe fields and measured in remanence, with the sample normal at  $\pm 65^\circ$  relative to the incident photon beam. This puts the in-plane remanent magnetization at a  $25^\circ$  or  $155^\circ$  angle with respect to the photon polarization. The photons were circularly polarized  $85 \pm 5\%$ ,<sup>6</sup> and consecutive spectra (about 5 min each) were taken at alternating incident angles. Absorption spectra are collected in the total electron yield mode, and were subsequently normalized to the total yield of a clean Cu(111) crystal over the same energy range.

Figure 1 shows the magnetization loop of a piece of the multilayer sample (as deposited) measured by superconducting quantum interference device (SQUID) magnetometry (note that about half the magnetization in this sample originates from the Fe buffer and overlayers). The magnetic behavior of the multilayer is distinct from that of an alloy with the same composition, since such alloys have a Curie temperature below  $200^\circ\text{C}$ .<sup>12</sup> This loop demonstrates the high remanent magnetization of this film (78%). The magnetization is normalized to the volume of Fe present in the sample, but the saturation magnetization ( $1450 \text{ emu}/\text{cm}^3$ ) is reduced from that of bulk Fe ( $1714 \text{ emu}/\text{cm}^3$ ). Taking into account the V magnetization (see below) one would expect a satura-

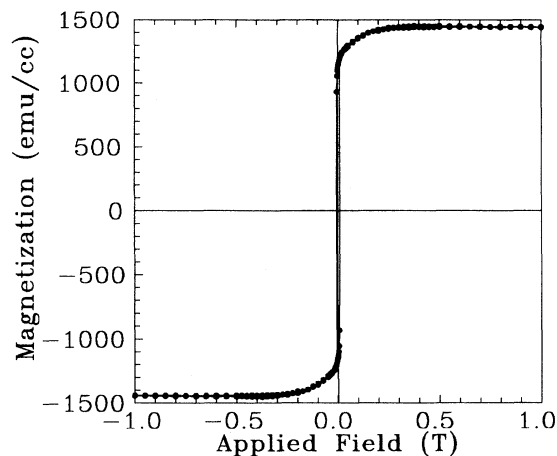


FIG. 1. SQUID magnetization loop of the Fe/V multilayer as grown, after air exposure. The magnetization axis is normalized to the volume of Fe in the film.

tion magnetization of  $<1640 \text{ emu/cm}^3$  because the V moments are aligned antiparallel to the Fe. Considering the experimental errors ( $\approx 10\%$ ), the measured magnetization is consistent with an assumption of the bulk magnetic moment on the Fe atoms.

Some surface oxidation was evidenced by a large O  $K_1$  edge at  $\approx 530 \text{ eV}$  immediately after insertion. The sample was then cleaned by Ar ion sputtering in  $4 \times 10^{-5}$  Torr Ar for 30 min at 1 kV incident beam energy with about  $5 \mu\text{A/cm}^2$  deposited current density. Inspection of the raw absorption data showed that the oxygen signal was reduced by a factor of  $\approx 15$ . Both Fe and V XMCD signals were present as inserted, but reduced by a factor of  $1/2$  (V) and  $2/3$  (Fe) from the postsputtered sample. This is roughly consistent with a  $30 \text{ \AA}$  oxide layer before sputtering, assuming a  $20 \text{ \AA}$  exponential probing depth for the XMCD. This implies that the sample surface layer was largely removed by sputtering, including the  $22 \text{ \AA}$  Fe capping layer, thus exposing the multilayer film underneath.

After sputtering, the  $\approx 15$ -fold decrease of the oxygen feature indicates a  $2 \text{ \AA}$  equivalent oxide layer. Although this oxide may account for up to  $\approx 10\%$  of the Fe and V absorption signal, the oxide should not appreciably alter the XMCD signal from the V or Fe spectra except in the unlikely event that it were highly magnetic. Measurements on more highly oxidized samples containing Fe and V generally show little or no XMCD, and the  $L_3$  absorption peaks of oxidized Fe and V are shifted to higher photon energy by  $1.5 \text{ eV}$  and  $3 \text{ eV}$ , respectively. In the present postsputtered film, the peak shapes at the Fe and V absorption edges were not distinguishable from those of clean Fe and V.

Figure 2 displays the x-ray absorption coefficients,  $\alpha_{\pm 65^\circ}$ , for the Fe/V multilayer, after sputter cleaning, in its two orientations with respect to the incident photon beam. The upper graph displays the absorption coefficient near the Fe  $L_{2,3}$  absorption edge, while the lower graph displays the absorption coefficient through the V  $L_{2,3}$  edge (to the left of the dashed vertical line) and the O  $K_1$  edge (right of the dashed line). Beneath the absorption spectra, the XMCD signal, de-

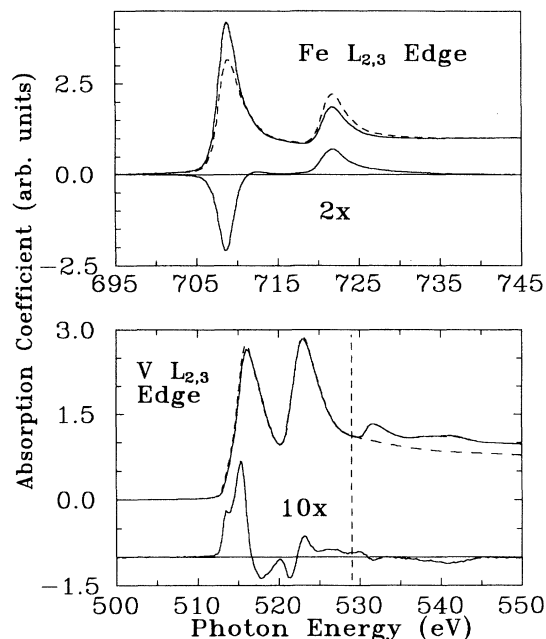


FIG. 2. X-ray absorption spectra,  $\alpha_{\pm 65^\circ}$ , from the Fe  $4.4 \text{ \AA}/\text{V } 3 \text{ \AA}$  multilayer taken using circularly polarized x rays incident at  $\pm 65^\circ$  relative to the sample normal. Spectra are displayed in the vicinity of the Fe and V  $L_{2,3}$  absorption edges. Above the V edge (to the right of the dashed vertical line) a weak oxygen  $K_1$  edge appears. The difference of these two spectra (XMCD) is presented below them on an expanded vertical scale.

finer as  $\alpha_{+65^\circ} - \alpha_{-65^\circ}$ , is plotted on an expanded vertical scale. The Fe and V spectra are normalized to one another such that far above the absorption edge they both have the same "edge jump." Because of the oxygen signal above  $530 \text{ eV}$ , it was necessary to extrapolate a background below the O edge to normalize the V signal. The approximate shape of the O edge was determined from spectra of more highly oxidized samples, and our estimated background is shown as a dashed line in the figure.

Both the Fe and V edges show significant XMCD. The absorption edge and XMCD of the Fe looks very similar to that found in epitaxial films,<sup>7</sup> and the magnitude of the XMCD signal is within  $10\%$  that observed for epitaxial films. This is consistent with the assumption of the bulk magnetic moment for the Fe atoms.

The magnitude of the V dichroism is much smaller than that of the Fe. We are unaware of previous measurements of the V dichroism, but the present measurement was highly reproducible (the displayed spectra are the average of 28 measurements). A very weak XMCD signal is also present in the vicinity of the O  $K_1$  edge. This is probably artificial, and due to the fact that the photon monochromator possesses strong absorption features at the O  $K$  edge, which reduces the reliability of intensity measurements in this region.

Note that at the onset of the  $L_3$  absorption edge, the Fe XMCD is negative, while the V XMCD is positive. This implies that in the multilayer, the induced V moments are aligned antiparallel with the Fe moments, in agreement with theoretical prediction<sup>4</sup> and similar to observations in thin-

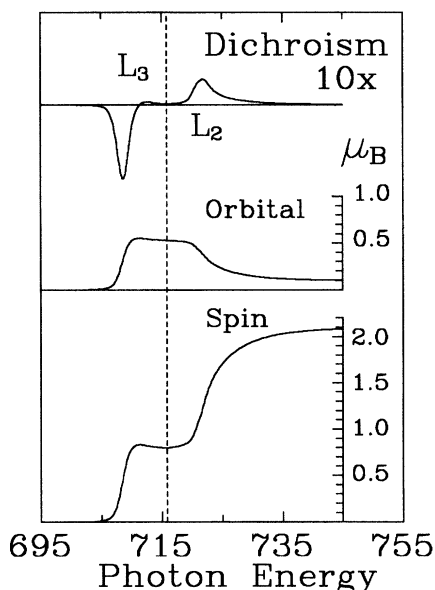


FIG. 3. The XMCD signal near the Fe  $L_{2,3}$  edge (top) is integrated following the prescriptions described in the text to determine the orbital (middle) and spin (bottom) magnetic moments associated with the Fe atoms. The end points of these integrals provide measures of the respective moments.

film experiments.<sup>5</sup> The Fe  $L_3$  XMCD signal peaks at the position of the Fe  $L_3$  absorption peak. Not so with the V, where the peak  $L_3$  XMCD signal occurs at slightly lower photon energy than the  $L_3$  peak. We find the XMCD from the V is relatively complex compared to the Fe. This fits in with a trend toward more structured XMCD spectra as one traverses the periodic table from right to left through the  $3d$  transition metals.<sup>7</sup>

This trend may be understood from the fact that the  $2p$  state of Fe has a large spin-orbit splitting (13 eV), hence exchange coupling (which is of order a few eV) does not affect the composition of the  $2p_{3/2}$  and  $2p_{1/2}$  states. In V, however, the spin-orbit splitting of the  $2p$  state is only 7 eV and the exchange coupling “remixes” the spin components of the  $2p_{3/2}$  and  $2p_{1/2}$  states. Thus, instead of a simple dichroism spectrum which is positive near the  $L_3$  edge and negative near the  $L_2$  edge, the V spectrum at, e.g., the  $L_3$  edge takes on some “ $L_2$ ” character, and has both positive and negative contributions. Such a picture is an oversimplification of the problem, but calculations for ionic atoms<sup>8</sup> show qualitatively the same kinds of changes in dichroism signal as the spin-orbit splitting is reduced.

To obtain quantitative information about the atomic magnetic moments of Fe and V, we apply so-called sum rules for the spin magnetic moment ( $2\langle S_z \rangle$ ) (Ref. 9) and orbital magnetic moment ( $\langle L_z \rangle$ ).<sup>10</sup> While the quantitative accuracy of these sum rules has been recently called into question,<sup>11,7</sup> it should still be possible to use Eqs. (1) and (2) to make *relative* comparisons between different elements when all have been measured using the same technique (XMCD).

For the present experiment, the sum rules take the form

$$\langle S_z \rangle \propto \int_{L_3} (\alpha_{+65} - \alpha_{-65}) - 2 \int_{L_2} (\alpha_{+65} - \alpha_{-65}), \quad (1)$$

and in the same units

$$\langle L_z \rangle \propto \frac{4}{3} \left( \int_{L_3} (\alpha_{+65} - \alpha_{-65}) + \int_{L_2} (\alpha_{+65} - \alpha_{-65}) \right). \quad (2)$$

The integrals represent the areas of the XMCD signal under the regions near the  $L_3$  and  $L_2$  absorption edges. In Fe, for example, the XMCD area under the  $L_3$  ( $L_2$ ) edge is negative (positive). Unfortunately, because of the relatively small spin-orbit splitting of the V  $2p$  level, it is not clear in the data exactly where the  $L_3$  edge ends and the  $L_2$  edge begins, necessary for the application of Eq. (1). Moreover, the spin “remixing” of the V core levels discussed above makes the application of Eq. (1) highly suspect. This problem can be observed in calculated spectra of atomic species,<sup>8</sup> where a relatively large spin moment is assumed for the calculation, but the application of Eq. (1) would obviously lead to a small value for  $\langle S_z \rangle$ . Therefore we shall regard Eq. (1) as providing only a lower limit for  $\langle S_z \rangle$  in V.

The results of the integrals (1) and (2) for Fe and V are shown in Figs. 3 and 4. We have normalized the Fe and V signals to the same constant, chosen such that the sum of the Fe spin and orbital moments is equal to  $2.18\mu_B$ , the bulk moment of Fe. For the V moment, our “transfer” of the Fe normalization constant is motivated by the fact that calculations of the nonresonant  $2p \rightarrow 3d$  transition probability is constant to within  $\approx 15\%$  for the  $3d$  transition metal elements.<sup>13</sup> This notion of transferability has been previously

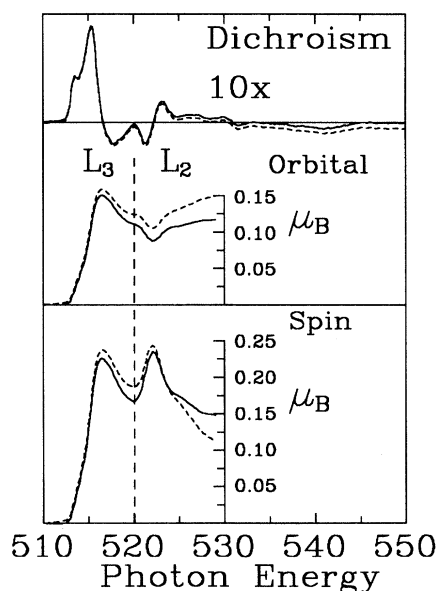


FIG. 4. As in Fig. 3, but for the XMCD signal near the V edge. Because of the proximity of the O  $K_1$  edge, the zero-dichroism base line above the V edge is difficult to determine and we show two results (solid and dashed curves) corresponding to the assumption of different backgrounds.

shown to be valid (to within 15%) between Ni and Co.<sup>13</sup> We estimate the assumption of transferability introduces an error of  $\approx \pm 25\%$  in the measurement of the total V moment.

In each figure, the dividing line between the  $L_3$  and  $L_2$  regions (needed for calculation of the spin moment) is shown by a dashed vertical line. As mentioned earlier, the structure in the monochromator transmission near the oxygen edge makes it difficult to establish the zero-dichroism base line on the high side of the V edge. For this reason, in the V case we show two results corresponding to the assumption of different zero-dichroism base lines above 530 eV.

From Figs. 3 and 4 we find the Fe magnetic moment is composed of an orbital part of  $0.10\mu_B$  and a spin part of  $2.08\mu_B$ . The V moment is similarly decomposed, with an orbital moment of  $0.13 \pm 0.04\mu_B$ , and a spin moment of at least  $0.13\mu_B$ . The sign (and to a lesser extent, the magnitude) of the measured V moment is consistent with the calculations of Ref. 4, which showed an induced V moment of  $0.23\mu_B$  aligned antiferromagnetically with Fe for 2 ML V layers sandwiched between Fe.

The results of Eqs. (2) and (1) indicate that the V orbital to spin moment ratio is near unity, much higher than in Ni (0.20), Co (0.16), or Fe (0.09) epitaxial films measured by the same technique.<sup>7</sup> However, if one compares orbital moments only, the values for Ni ( $0.15\mu_B$ ), Co ( $0.40\mu_B$ ), and Fe ( $0.32\mu_B$ ) are quite similar to that for V ( $0.13\mu_B$ ). This would indicate that the estimate of the V spin moment by Eq. (1) is indeed low, conceivably by as much as a factor of 10.

Such a result cannot be ruled out by the magnetization data, since the V comprises a rather small component of the total film.

In the present film, the Fe orbital moment ( $0.10\mu_B$ ) is reduced relative to its value in epitaxial Fe. This could be an indication of hybridization of the Fe and V wave functions where the electrons associated with the Fe acquire some of the character (orbital moment) associated with the V electrons. Such a conclusion is supported by the calculations,<sup>4</sup> which indicate a reduced Fe magnetic moment for Fe atoms at the Fe/V interface.

In conclusion, we have measured XMCD from a number of Fe/V structures, focusing on an Fe 4.4 Å/V 3 Å multilayer. The total Fe magnetic moment was near that of bulk Fe, as measured by XMCD, and confirmed by SQUID magnetometry. The presence of the O  $K_1$  edge complicates measurement of the V XMCD, whose magnetic moment was determined to be  $>0.26\mu_B$ , aligned antiferromagnetically with the Fe. The V orbital moment ( $0.13\mu_B$ ) is similar to that observed in ferromagnetic Fe, Co, and Ni. For the V spin moment, only a lower bound could be determined ( $0.13\mu_B$ ), and the actual value is likely to be higher.

The authors gratefully acknowledge K. P. Roche for technical support. This work was partially supported by the Office of Naval Research. The Synchrotron Radiation Center is supported by NSF under Grant No. DMR-9212658.

\*Present address: Dept. of Physics and Astronomy, Ohio University, Athens, OH 45701.

<sup>1</sup>S. S. P. Parkin, in *Ultra-thin Magnetic Structures*, edited by B. Heinrich and J. A. C. Bland (Springer-Verlag, Berlin, 1994), Vol. 2.

<sup>2</sup>For an elegant counterexample to this statement, see C. Turtur and G. Bayreuther, Phys. Rev. Lett. **72**, 1557 (1994).

<sup>3</sup>S. S. P. Parkin, Phys. Rev. Lett. **67**, 3598 (1991).

<sup>4</sup>A. Vega, A. Rubio, L. C. Balbas, J. Dorantes-Davila, S. Bouarab, C. Demangeat, A. Mokrani, and H. Dreyse, J. Appl. Phys. **69**, 4544 (1991).

<sup>5</sup>T. G. Walker and H. Hopster, Phys. Rev. B **49**, 7687 (1994).

<sup>6</sup>R. W. C. Hansen, W. L. O'Brien, and B. P. Tonner, Nucl. Instrum. Methods (to be published).

<sup>7</sup>W. L. O'Brien, B. P. Tonner, G. R. Harp, and S. S. P. Parkin, J.

Appl. Phys. **76**, 6462 (1994); W. L. O'Brien and B. P. Tonner, Phys. Rev. B **51**, 617 (1995).

<sup>8</sup>G. van der Laan and B. T. Thole, Phys. Rev. B **43**, 13 401 (1991).

<sup>9</sup>Paolo Carra, B. T. Thole, Massimo Altarelli, and Xindong Wang, Phys. Rev. Lett. **70**, 694 (1993).

<sup>10</sup>B. T. Thole, Paolo Carra, F. Sette, and G. van der Laan, Phys. Rev. Lett. **68**, 1943 (1992).

<sup>11</sup>R. Wu, D. Wang, and A. J. Freeman, Phys. Rev. Lett. **71**, 3581 (1993).

<sup>12</sup>K. Adachi, in *3d, 4d, and 5d Elements, Alloys, and Compounds*, edited by H. P. J. Wijn, Landolt-Börnstein, New Series, Group 3, Vol. 19, Pt. a (Springer-Verlag, Berlin, 1986).

<sup>13</sup>M. G. Samant, J. Stöhr, S. S. P. Parkin, G. A. Held, B. D. Hermsmeier, F. Herman, M. van Schilfgaarde, L. C. Duda, D. C. Mancini, N. Wassdahl, and R. Nakajima, Phys. Rev. Lett. **72**, 1112 (1994); J. Stöhr (private communication).